31st Congress of the International Council of the Aeronautical Sciences
Belo Horizonte, Brazil; September 09-14, 2018

INVESTIGATION ON AERO-PROPULSIVE BALANCE FOR HIGH-SPEED POWERED EXPERIMENTAL FLIGHT TEST VEHICLE WITHIN THE HEXAFLY-INT PROJECT

A.A. Gubanov*, D.S. Ivanyushkin*, N.V. Kukshinov, A.N. Prokhorov**, V.A. Talyzin*, N.V. Voevodenko***
*** Central Aerohydrodynamic Institute named after Professor N.E. Zhukovsky (TsAGI), Russian Federation, ** Central Institute of Aviation Motors named after P.I. Baranov (CIAM), Russian Federation**

Keywords: *scramjet, HEXAFLY-INT, aero-propulsive balance, CFD, ground tests*

Abstract

The results of computational and experimental studies of the aero-propulsive balance of the high-speed experimental flight test vehicle EFTV carried out within the framework of the HEXAFLY-INT project are presented in the paper. Three-dimensional numerical modeling of the flow around the EFTV and the flow of the hydrogen-air mixture in the internal flow path in a wide range of angles of attack and equivalence ratios was performed. The forces acting on separate parts of the EFTV and on the EFTV as a whole are determined. The results of experiments on the flow around a scaled aerodynamic model of the EFTV and on the study of the working process in the combustion chamber of the scramjet facility module are presented. Estimations of the realizability of the aero-propulsive balance of the presented configuration of the flying vehicle.

1 Introduction

In the HEXAFLY project, a scale model of a hypersonic civil aircraft was proposed, the cruise flight of which is carried out at a speed corresponding to the Mach number M = 7.5 [1-2]. The concept of this model formed the basis of the high-speed experimental flight test vehicle EFTV studied within the framework of the HEXAFLY-INT project [3]. The configration of the EFTV is shown in Fig. 1. TsAGI and CIAM are carrying out work on this project in the area of calculating and experimental studies of external aerodynamics, the operation of the air intake device and the thrust characteristics of the hydrogen scramjet. For these purposes, a lot of numerical calculations have been performed and several experimental models have been made for testing at various facilities.

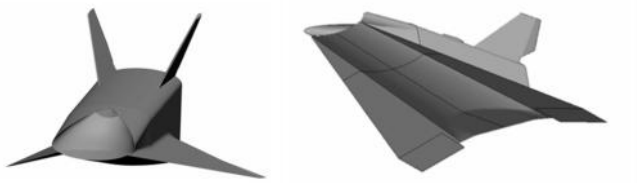

Fig. 1. Configuration of the EFTV HEXAFLY

Fig. 2 shows a photograph of the aerodynamic model for testing in the T-116 wind tunnel in TsAGI and the scramjet facility module for testing at the C-16VK facility in CIAM. The aerodynamic model having a length of 1 m was made at a scale of 0.35 of the actual size of the EFTV, and the full-size facility module is 3 m length.

2 Investigation of the EFTV intake

A model of the EFTV powered option was made with the internal duct to investigate the intake characteristics and to take into account the influence of the engine duct on external aerodynamics of the vehicle. Composition of the model and the photo of the model installed in

the test section of the wind tunnel T-116 are shown in Fig. 3.

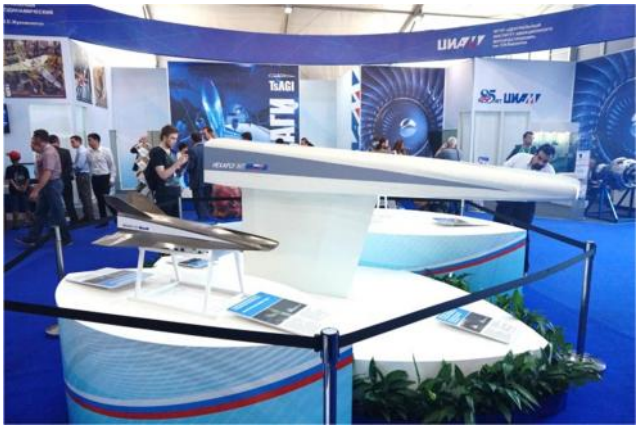

Fig. 2. The EFTV aerodynamic model and the full-scale scramjet facility module at MAKS-2015 exhibition, Zhukovsky 2015

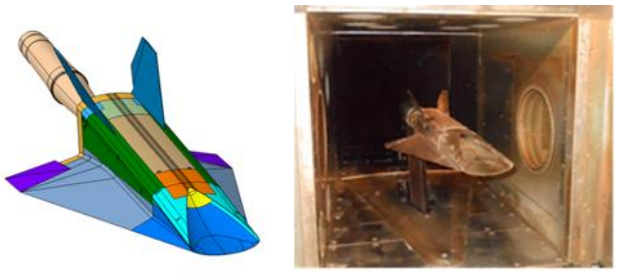

Fig. 3. Composition of the aerodynamic model, EFTV powered option (left) and photo of the model installed in the test section of TsAGI T-116 wind tunnel (right)

The model was made with the internal duct simulating the intake configuration up to its throat. The other parts of the duct were modified as compared to the real engine components. At some distance from the intake throat, the duct was made with the expanding, and then with constant cross-sectional area. The nozzle of the model duct was composed of two parts with contracting and constant cross-sectional areas ensuring a uniform exit flow with sonic velocity. Such a configuration of the internal duct allows determining the intake mass flow rate and the nozzle exit flow momentum by measuring total and static pressures and total temperature in the exit section of the nozzle by the special rake consisting of several total and static pressure probes and thermocouples. Configuration of the internal duct of the model and position of the measurement rake are shown in Fig. 4.

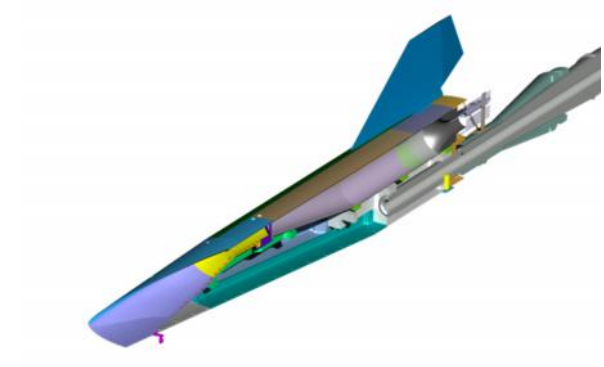

Fig. 4. Configuration of the internal duct of the model and the measurement rake

In order to study the influence of the intake throat area on the intake starting performance, the model was produced with two variants of the intake throat: the original one corresponding to the EFTV configuration with the contraction ratio CR = 8.6, and a more expanded throat with CR = 7.4 (CR being the ratio of the intake capturing area to the area of the intake throat). These two variants of the intake throat were ensured by two replaceable inserts shown in Figs. 3 and 4 by yellow color.

The results of tests presented, in particular, Refs. [4] and [5]showed that start of the intake depends from both the intake contracting ratio CR and the boundary layer (BL) state on the intake surface. The intake in the wind tunnel T-116 started just with the expanded throat area, and installation of transition grit ensuring BL tripping on the intake surface significantly improved the intake starting performance. The results of tests in terms of the intake mass flow rate f dependencies from angle-of-attack of the model α obtained at Mach numbers 7 and 8 with different variants of BL tripping grits are shown on Fig. 5.

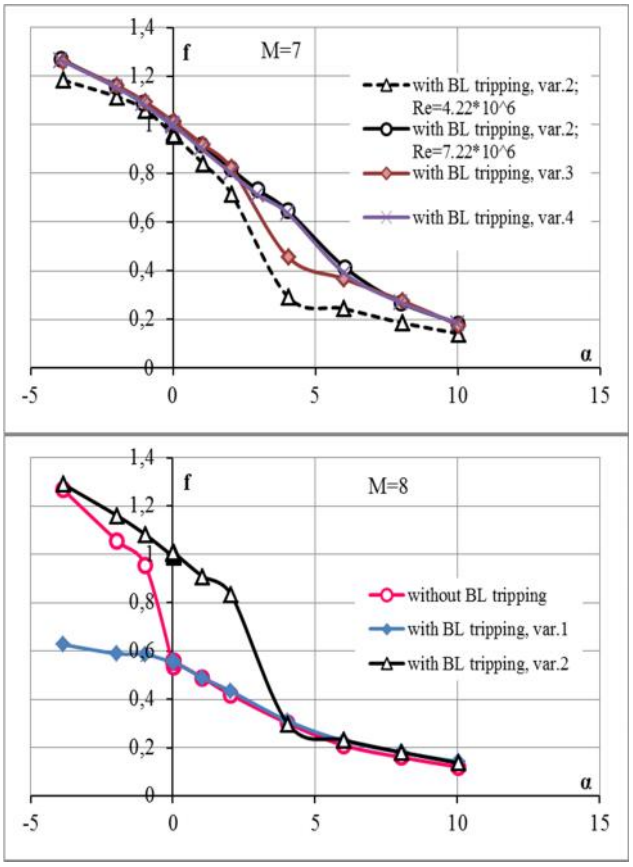

Fig.5.Experimental data on the intake mass flow rate coefficient *f* vs. angle-of-attack α at M = 7 and 8

The main test results on external characteristics of the model were obtained with the expanded intake throat area (CR = 7.4) and with the BL tripping grit, variant 2 consisting of 10 screw heads of countersunk shape with a height of 1.2 mm and 3.8 mm top diameter installed at distances of approximately 15 mm and 35 mm from the leading edge of the intake at three positions dispersed by the lateral co-ordinate. The test results obtained at Mach number M=7 and 8 for drag force coefficient C_D, lift force coefficient C_L, aerodynamic efficiency L/D, and pitching moment coefficient C_m are presented in Figs. 6 and 7.

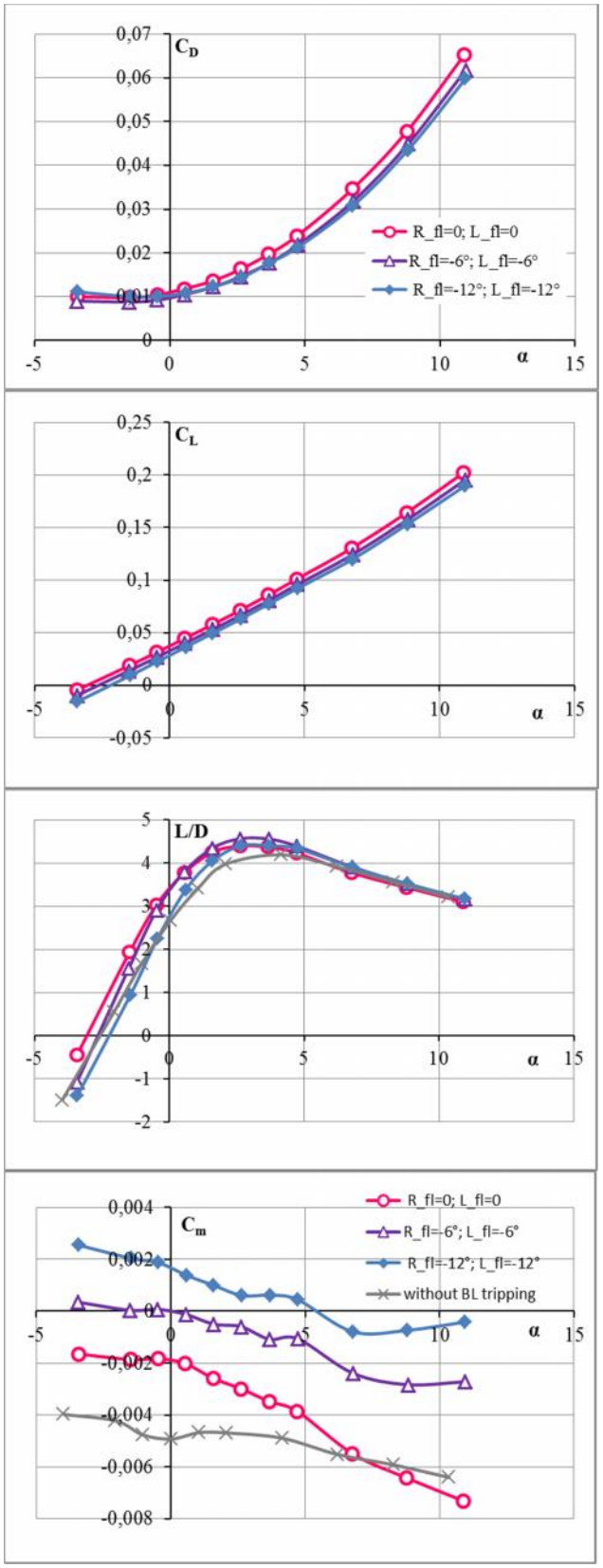

Fig. 6. Experimental data on external aerodynamic characteristics of the EFTV powered concept model at M = 7: drag force coefficient C_D, lift force coefficient C_L, aerodynamic efficiency L/D, and pitching moment coefficient C_m vs. angle-of-attack α

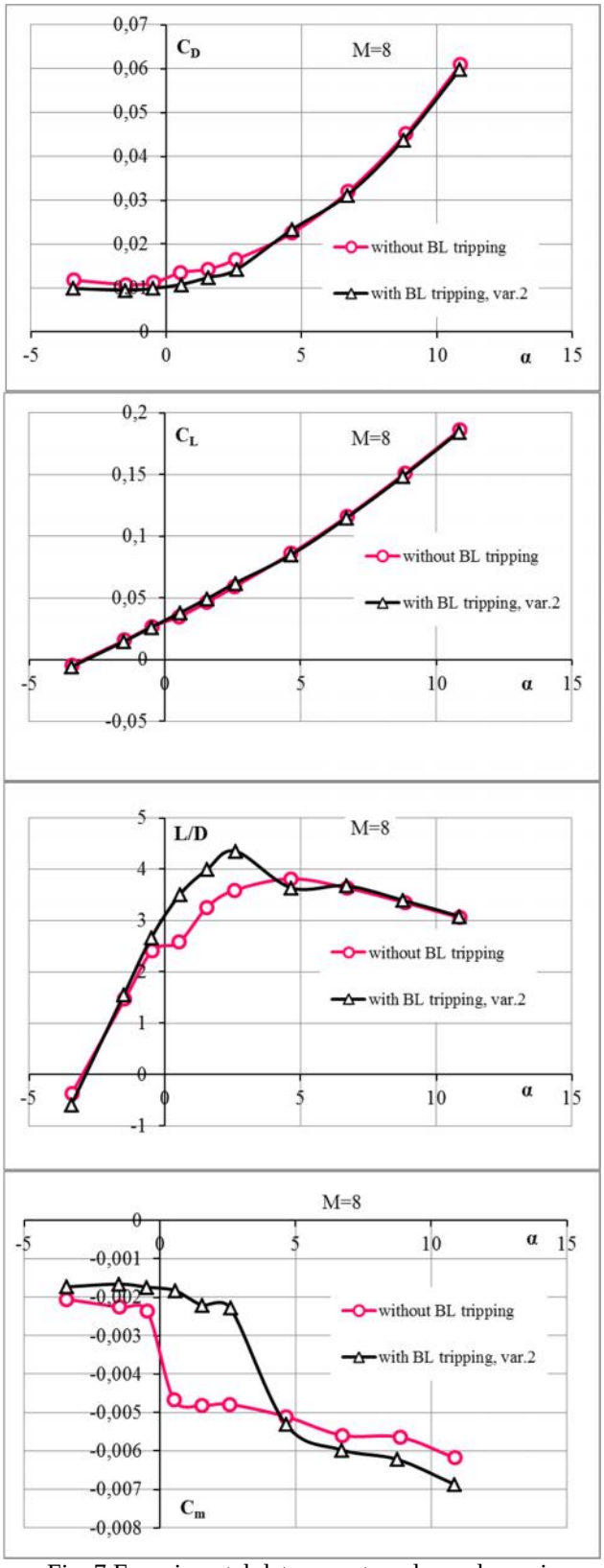

Fig. 7.Experimental data on external aerodynamic characteristics of the EFTV powered concept model at M = 8: drag force coefficient C_D, lift force coefficient C_L, aerodynamic efficiency L/D, and pitching moment coefficient C_m vs. angle-of-attack α

3 Aerodynamic characteristics of the EFTV

The main aerodynamic characteristics of the EFTV model were C_D- drag force coefficient, C_L- lift force coefficient, L/D- aerodynamic efficiency and the f - the intake mass-flow rate coefficient. CFD calculations were performed in a three-dimensional formulation with the solution of the Reynolds-averaged Navier-Stokes equations for a wide range of angles of attack at the Reynolds number Re = $3.7*10^6$. Experiments, as mentioned above, were carried out in the wind tunnel T-116. Fig. 8 shows the dependencies of the above aerodynamic characteristics on the angle of attack α. Aerodynamic efficiency has a maximum in the range of angles of attack α = 2˚¬ 4˚. For C_D and C_L, the calculated and experimental results are satisfactorily corresponded in the entire range of angles of attack. With an increase of Reynolds number, the drag force coefficient C_D decreases, and this leads to an increase in the aerodynamic efficiency L/D. The presence of vortex generators and the Reynolds number of the oncoming flow have a significant effect on the mass-flow rate coefficient f. It can be seen that the experimental data for the case without a forced laminar-turbulent transition on the compression surfaces of the intake are in the region below the calculated one. This indicates that in this case the flow in the intake is more laminar. In the case of experiments with vortex generators increasing angle of attack leads to unstart of the air intake. Comparing the results of experiments with vortex generators with different Reynolds numbers of the oncoming flow, it should be noted that as the Reynolds number increases, the unstarting of the shifts towards large angles of attack: as can be seen from the experimental dependences of the mass-flow rate coefficient on the angle of attack (Fig. 8), in the case Re = $7*10^6$ this happens at α = 3˚ ¬ - 4˚, and in the case of Re = $4*10^6$ - much earlier.

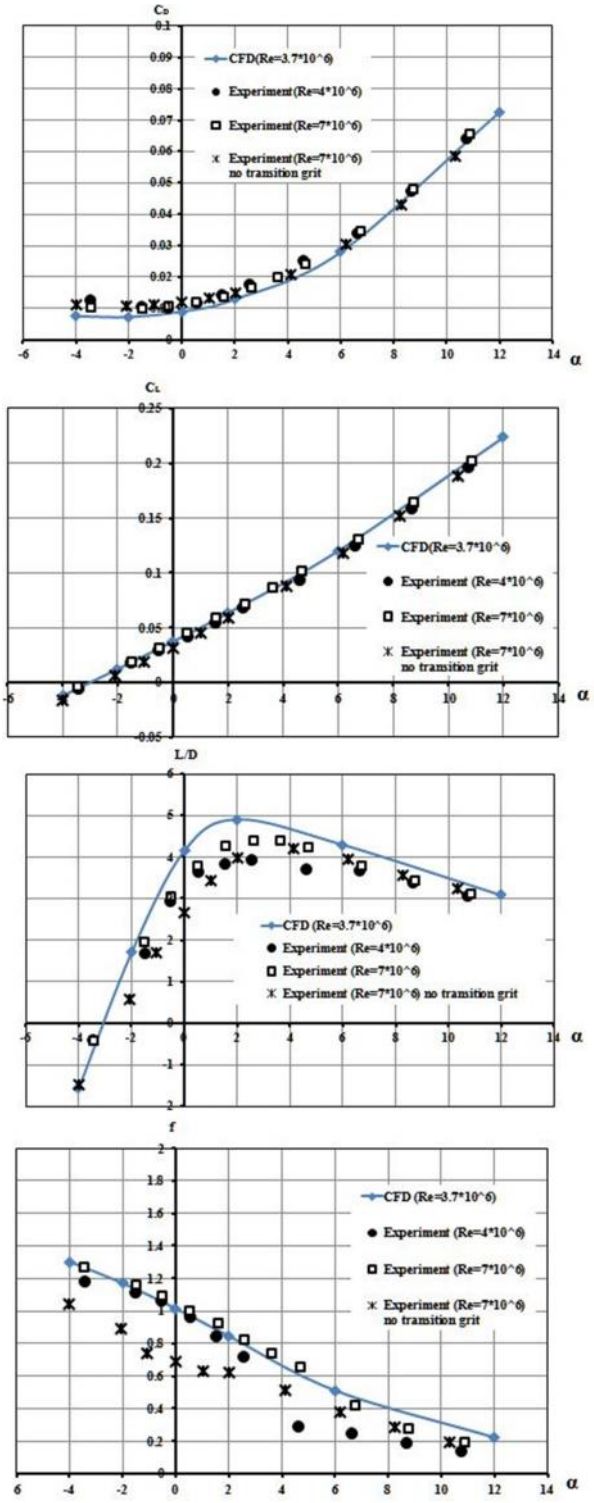

Fig.8.Numerical and experimental data on external aerodynamic characteristics of the EFTV powered concept model at M = 7: drag force coefficient C_D, lift force coefficient C_L, aerodynamic efficiency L/D, and the intake mass flow rate coefficient *f* vs. angle-of-attack α

The obtained data were used to determine the resultant forces acting on the EFTV during the operation of the scramjet.

4 Aero-propulsive balance of the EFTV

The thrust characteristics of the EFTV scramjet were determined both numerically and experimentally. Defined characteristics were engine thrust, specific impulse and combustion efficiency. From the values of these quantities one can draw conclusions about the efficiency of the scramjet and the realizability of the aero-propulsive balance. Positive aero-propulsive balance means the excess of thrust created by the engine, over the external aerodynamic drag of the vehicle.

In numerical simulation, the task of the flow of a viscous chemically reacting gas was solved. Details of the results and methods used can be found in [6-7]. The forces and moments acting on the flow path of the engine during the flow of air without fuel supply and with fuel supply in the range of equivalence ratios ER = 0.8 - 1.2 were determined in a wide range of angles of attack. Integration of these results with the results of calculation of external aerodynamics made it possible to evaluate the aero-propulsive balance of the EFTV based on the results of numerical simulation.

For the experimental determination of the thrust characteristics of the scramjet in CIAM a facility module was created (Fig. 9). It is a scramjet integrated with the intake and installed on a power pylon. There are no external aerodynamic surfaces (wings, elevons and ailerons). In comparison with the original modification (Fig. 1), the facility module has a technological intake which provides a similar flow structure and the same integral values of the main parameters as the original intake [8-9]. The facility module tests were carried out at the C-16VK facility in CIAM. During tests equivalence ratios and fuel flow-rates through the fuel supply bands were varied. A total of 18 runs were carried out, with the total pressure and the total temperature of the oncoming flow being respectively p * = 6.1 - 6.5 MPa and T * = 2310 K. The experiments were carried out with the installation of the facility module at an angle of attack α = -2 °. Details are presented in [10].

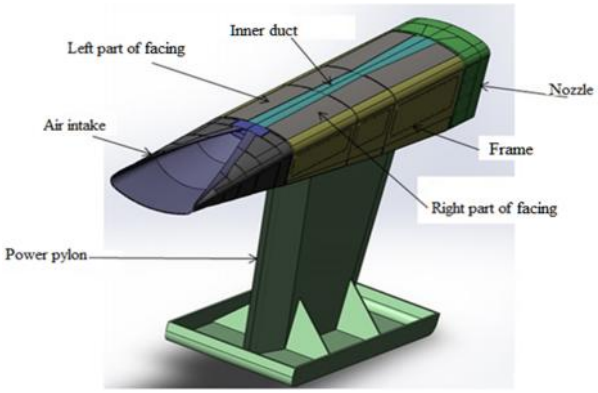

Fig.9.Scramjet facility module of EFTV

Dependences of the resulting longitudinal force coefficient C_R and lift force coefficient C_L on the angle of attack for different modes of engine operation are shown in Fig. 10.

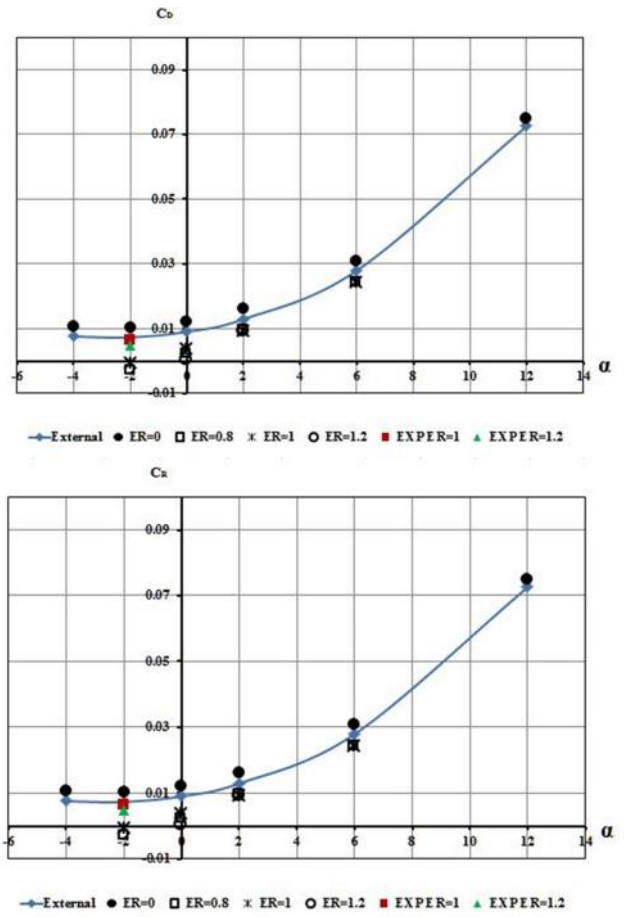

Fig.10.Numerical and experimental data on external aerodynamic characteristics of the EFTV powered concept model at M = 7with scramjet operation: resulting force coefficient C_R, lift force coefficient C_L

The blue lines on the graphs show the values of the external aerodynamic drag coefficients (without taking into account the compression surface of the air intake device and the elements of the internal flow path). The black dots show the values of the coefficients C_R and C_L, which were calculated at different coefficients ER = 0, 0.8, 1, 1.2. Red square and green triangle are experimental points for ER = 1 and ER = 1.2 respectively. Positive aero-propulsive balance leads to the C_R value position in the negative area. As can be seen from all the cases considered, this condition is satisfied by the values of C_R at the angle of attack α = -2 ° and ER = 0.8; 1. At the same time, the same parameters specified in the experiment did not allow obtaining a positive aero-propulsion balance.

It is necessary to describe in detail the method for determining C_R from the results of calculations and experiments. The coefficient C_R in was determined by the formula (1).

$$C_R = \frac{F_R}{\frac{1}{2} \cdot \rho_\infty \cdot w_\infty^2 \cdot S_{ref}} \qquad (1)$$

where F_R - longitudinal force, ρ_∞ - density of the oncoming flow, w_∞-speed of the oncoming flow, S_{ref} - characteristic area of the intake entrance.

In calculations, the value of the force F_R is determined directly as the integral of the pressure on the area. The walls of the model are divided into parts, so you can determine the contribution to the resulting longitudinal force F_R and accordingly the coefficient C_R for each element of the flow path and the outer region of the EFTV.

The experimental values of C_R were obtained as follows. In the experiments, the longitudinal force acting on the facility module was measured. The flow of the module occurs both before the fuel supply to the combustion chamber and during the supply, while constant values of the parameters of the oncoming flow are maintained. Thus, the force sensor before the fuel supply shows the total aerodynamic drag of the facility module, and during the fuel supply an effective thrust. Assuming that the external drag of the facility module and the flow structure in the air intake do not change in run

while the oncoming flow are maintained the thrust can be determined by formula (2).

$$T = \Delta R - I_{\infty} + I_{out\_c} \qquad (2)$$

where T is the thrust of the engine, ΔR is the experimentally determined difference in the readings of the force sensor when the fuel is supplied and without supply, I_{∞} is the oncoming flow impulse, I_{out_c} is the flow impulse at the nozzle exit of the facility module without fuel supply (determined from three-dimensional numerical simulation).

Further, obtained from (2) T is substituted as F_R in (1). The resulting C_R is the additional coefficient of longitudinal force (or the engine thrust coefficient), which has a negative value in the adopted designation system, should be added to the external drag of EFTV with the internal flow path (black circles in Figure 10).

In the experiments the values of the ER coefficient were varied which had a significant effect on the EFTV aero-propulsive balance. Fig. 11 shows the dependence of C_R on ER.

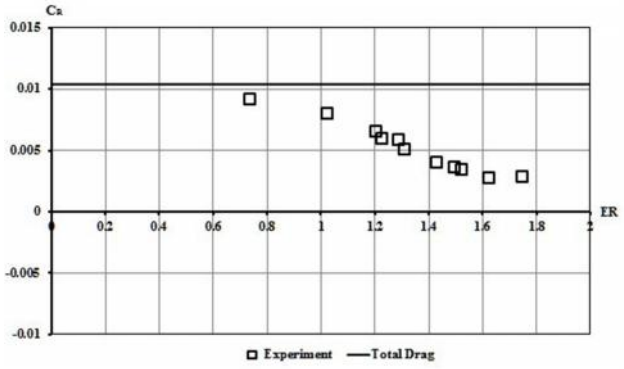

Fig.11.Experimental resulting force coefficient C_R of the EFTV powered concept at M = 7with scramjet operation

As can be seen from the graph with increasing ER the value of the C_R decreases due to the increase in thrust created by the engine. But even at plenty high values of the ER a positive aero-propulsive balance is not observed, the minimum value of the coefficient is C_R = 0.00267 at ER = 1.629. It should be noted that this value of C_R is relatively small and close to the balance. It was shown in [10] that the combustion efficiency in the experiments did not exceed η = 0.6 at the maximum ER. Even a slight increase of the combustion efficiency due to an improvement in the quality of the working process in the combustion chamber will lead to a positive aero-propulsive balance of EFTV, so it can be said that the proposed configuration is capable of providing a positive aero-propulsive balance.

5 Conclusions

Aero-propulsive balance of high-speed experimental flight test vehicle EFTV was investigated. Three-dimensional numerical simulation of the EFTV flow around and the flow in the inner flow path was carried out. The aerodynamic model of EFTV was tested in wind tunnel T-116 in TsAGI. The aerodynamic characteristics of EFTV in a wide range of angles of attack are determined. Numerical simulation of the combustion of a hydrogen-air fuel mixture in the combustion chamber of EFTV integrated with the he intake over a wide range of angles of attack and the equivalence ratios ER was carried out. The limits of the operability of the proposed scramjet configuration were shown and the coefficients of forces acting on the apparatus are determined. Experimental studies of HEXAFLY-INT facility module were carried out in high-enthalpy facility in CIAM. Thrust characteristics of the facility module were determined. Taking into account the numerical and experimental results obtained for the engine running case the values of resulting longitudinal force coefficient C_R were obtained. It has been calculated that the positive aero-propulsive balance is realized at the angle of attack α = -2 ° and the values of ER = 0.8 and 1. Experimentally positive aero-propulsive balance for EFTV taking into account all external aerodynamic surfaces when integrating the test results of the scramjet facility module and calculations of EFTV external aerodynamics was not demonstrated. Although the result was very close to achieving this balance: the smallest value of the coefficient C_R = 0.00267 with ER = 1.629; wherein C_R = 0.010412 with ER = 0 (without supplying fuel).

Acknowledgements

This work was performed within the ‘High Speed Experimental Fly Vehicles - International’ (HEXAFLY-INT) project

fostering International Cooperation on Civil High-Speed Air Transport Research. HEXAFLY-INT, coordinated by ESA-ESTEC, is supported by the EU within the 7th Framework Program Theme 7 Transport, Contract no.: ACP3-GA-2014-620327. The project is also supported by the Ministry of Industry and Trade, Russian Federation. Further information on HEXAFLY-INT can be found on http://www.esa.int/techresources/hexafly_int.

References

[1] Steelant J., Langener T., Hannemann K, Riehmer J., Kuhn M., Dittert C., Jung W., Marini M., Pezzella G., Cicala M., Serre L. Conceptual Design of the High-Speed Propelled Experimental Flight Test Vehicle HEXAFLY. *20th AIAA International Space Planes and Hypersonic Systems and Technologies Conference*. Glasgow, Scotland, July 6-9, 2015: AIAA-2015-3539.

[2] Steelant J., Varvill R., Defoort S., Hannemann K. Marini M. Achivements obtained for sustained hypersonic flight within the LAPCAT-II project. *20th AIAA International Space Planes and Hypersonic Systems and Technologies Conference*. Glasgow, Scotland, July 6-9, 2015: AIAA-2015-3677.

[3] Steelant J., Marini M., Pezella G., Reimann B., Chernyshev S.L., Gubanov A.A., Talyzin V.A., Voevodenko N.V., Kukshinov N.V., Prokhorov A.N., Neely A.J., Kenell C., Verstraete D., Buttsworth D. Numerical and Experimental Research on Aerodynamics of High-Speed Passenger Vehicle within the HEXAFLY-INT Project. *30th Congress of the International Council of the Aeronautical Sciences (ICAS)*. Daegeon, Korea, September 26-30, 2016: ICAS-2016-0353.

[4] Voevodenko N.V., Gubanov A.A., Ivaniushkin D.S., Lunin V.Yu., Gusev D.Yu., Ivankin M.A., Talyzin V.A., and Yakovleva, V.A. Numerical and experimental studies of the flow on HEXAFLY-INT experimental flight test vehicle air intake. *20th AIAA International Space Planes and Hypersonic Systems and Technologies Conference*. Glasgow, Scotland, July 6-9, 2015: AIAA-2015-3584.

[5] Voevodenko N.V., Gubanov A.A., Gusev D.Yu., Ivankin M.A., Ivanyushkin D.S., Lunin V.Yu., Meshennikov P.A., Talyzin V.A., Shvalev Yu.G., Yakovleva V.A. Boundary layer state influence on start of the inward-turning intake. *30th Congress of the International Council of the Aeronautical Sciences (ICAS)*. Daegeon, Korea, September 26-30, 2016: ICAS-2016-0383.

[6] Batura S.N., Gouskov O.V., Kukshinov N.V. Computational research of operation process in the combustion chamber of HEXAFLY-INT model in wide range of free stream conditions and equivalence ratios. 7th European Conference for Aeronautics and Space Sciences, Milan, Italy, July 3-6, 2017: Paper № 454.

[7] Kukshinov N.V., Batura S.N., Gouskov O.V., Prokhorov A.N. Numerical study of hydrogen mixing and combustion in HEXAFLY-INT combustion chamber. *7th Space Propulsion Conference*. Sevilla, Spain, May 14-18, 2018: Paper SP2018_570.

[8] Aleksandrov V.Yu., Danilov M.K., Gouskov O.V., Gusev S.V., Kukshinov N.V., Prokhorov A.N., Zakharov V.S. Numerical and experimental investigation of different intake configurations of HEXAFLY-INT facility module. *30th Congress of the International Council of the Aeronautical Sciences (ICAS)*. Daegeon, Korea, September 26-30, 2016: ICAS-2016-0380.

[9] Karl S., Steelant, J., Cross-Flow Phenomena in Streamline Traced Hypersonic Intakes. *20th AIAA International Space Planes and Hypersonic Systems and Technologies Conference*. Glasgow, Scotland, July 6-9, 2015: AIAA-2015-3594.

[10] Aleksandrov V.Yu., Kukshinov N.V., Prokhorov A.N., Rudinskiy A.V. Analysis of the integral characteristics of HEXAFLY-INT facility module. *21st AIAA International Space Planes and Hypersonic Systems and Technologies Conference*. Xiamen, China, March 6-9, 2017: AIAA-2017-2179.

Contact Author Email Address

The contact author is Nikolay Kukshinov, CIAM, e-mail: kukshinov@ciam.ru

Copyright Statement